Miscibility Gap in Fe-Ni-Al and Fe-Ni-Al-Co Systems

SHI MING HAO, T. TAKAYAMA, K. ISHIDA, and T. NISHIZAWA

The phase equilibria in Fe-Ni-Al and Fe-Ni-Al-Co systems have been investigated by the diffusion couple technique, and the miscibility gap that separates α_1 (Fe-rich disordered bcc phase) from α_2 (NiAl-rich ordered bcc phase) has been determined. It has been ascertained that the three-dimensional shape of the miscibility gap is not simple helmetlike, but has a peculiar ridge at the order-disorder transition temperature. The miscibility gap is narrowed and shifted to the Fe-rich corner by the addition of Co, and Co atoms are distributed to the α_2 rather than the α_1. Furthermore, by alloying Co, the fcc γ phase is stabilized and the miscibility gap between α_1 and α_2 is hidden to some extent by the phase regions concerned with the γ phase.

I. INTRODUCTION

THE phase diagrams of Fe-Ni-Al and Fe-Ni-Al-Co systems have a practical importance for the developments of Alnico magnets, PH stainless steels, and maraging steels. In particular, the miscibility gap in these systems has a key role on the properties of Alnico magnets, and it has been established that the high coercivity of Alnico alloys primarily results from the breakdown of a high temperature bcc phase α into two bcc phases of Fe-rich disordered α_1 and NiAl-rich ordered α_2.

The miscibility gap in the broad bcc phase that extends from the Fe corner to the NiAl in Fe-Ni-Al system was first detected by Kiuchi[1] and Bradley and Taylor,[2,3] independently. A reexamination of the phase diagram of the system was done by Bradley,[4] who determined the $\alpha_1 + \gamma$ and $\alpha_1 + \alpha_2$ phase regions by microscopic studies. The isothermal and vertical section diagrams by Bradley are reproduced in Figures 1 and 2, where the vertical section is taken through the line XY in Figure 1 to avoid the appearance of the fcc γ phase. The diagram for the pseudo-binary Fe-NiAl system was presented by Marcon *et al.*[5]

There are two interesting features in the form of $\alpha_1 + \alpha_2$ phase region in Bradley's diagram. One is the fact that the region is a "closed miscibility gap" or "miscibility gap island", because the miscibility gap does not appear in the bcc phase in Fe-Ni, Ni-Al, and Fe-Al binaries. Another is the abnormal shape of the vertical section of the miscibility gap with a horn extending toward the solidus curve. The first phenomenon has been analyzed thermodynamically by Meijering,[6] who showed that the possibility of formation of "miscibility gap island" by using the regular solution model. As shown in Figure 2, however, there is a great discrepancy between the observed miscibility gap and the one estimated by Meijering's theory. To explain this inconsistency, Hardy[7] introduced the effect of order-disorder reaction on the miscibility gap, and succeeded to account for the general mode of the miscibility gap in Fe-NiAl pseudo-binary system.

A simple and explicit treatment of the effect of ordering and magnetic transition on the phase equilibria has been developed by the present authors;[8,9] this treatment permits us to calculate the miscibility gap over the whole range of compositions in ternary systems. The calculation predicts that the summit temperature of miscibility gap is raised to a

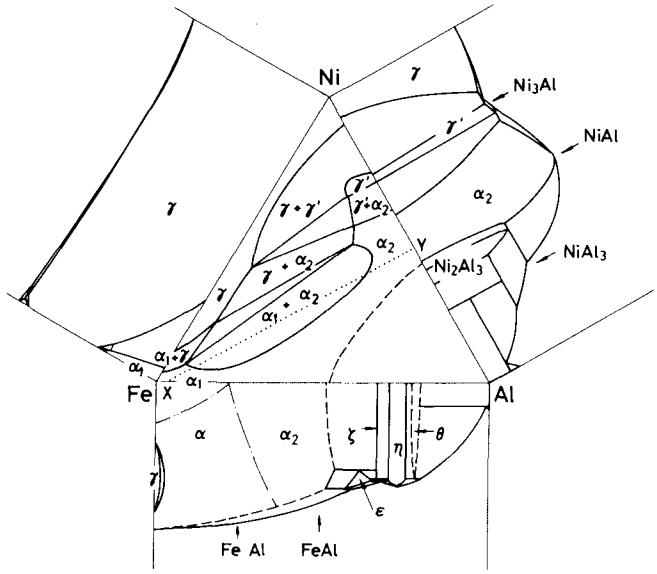

Fig. 1—Phase equilibria in Fe-Ni side of Fe-Ni-Al system at 750 °C by Bradley.

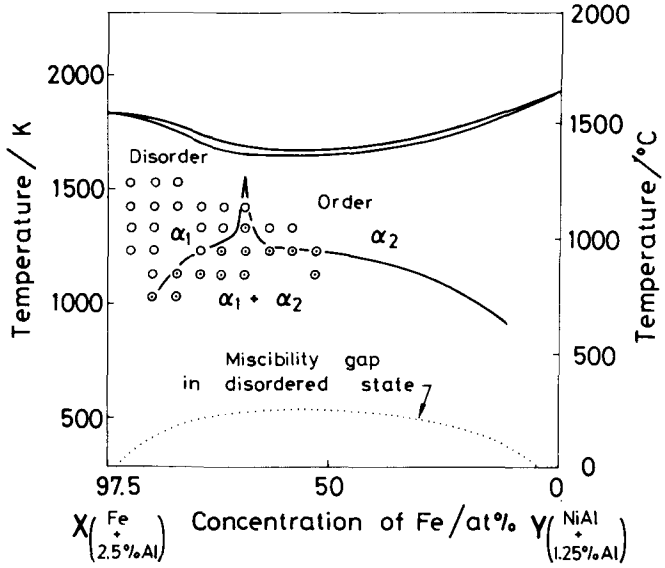

Fig. 2—Vertical section diagram of Fe-Ni-Al system by Bradley. Dotted line shows the miscibility gap calculated by the regular solution model.

SHI MING HAO is a Lecturer, Northeast Institute of Technology, Schenyang, China. T. TAKAYAMA is a Senior Engineer, Manufacturing Engineering Research Center, Komatsu Ltd., Hirakata, Japan. K. ISHIDA, Associate Professor, and T. NISHIZAWA, Professor, are with the Department of Materials Science, Faculty of Engineering, Tohoku University, Sendai 980, Japan.

Manuscript submitted March 29, 1984.

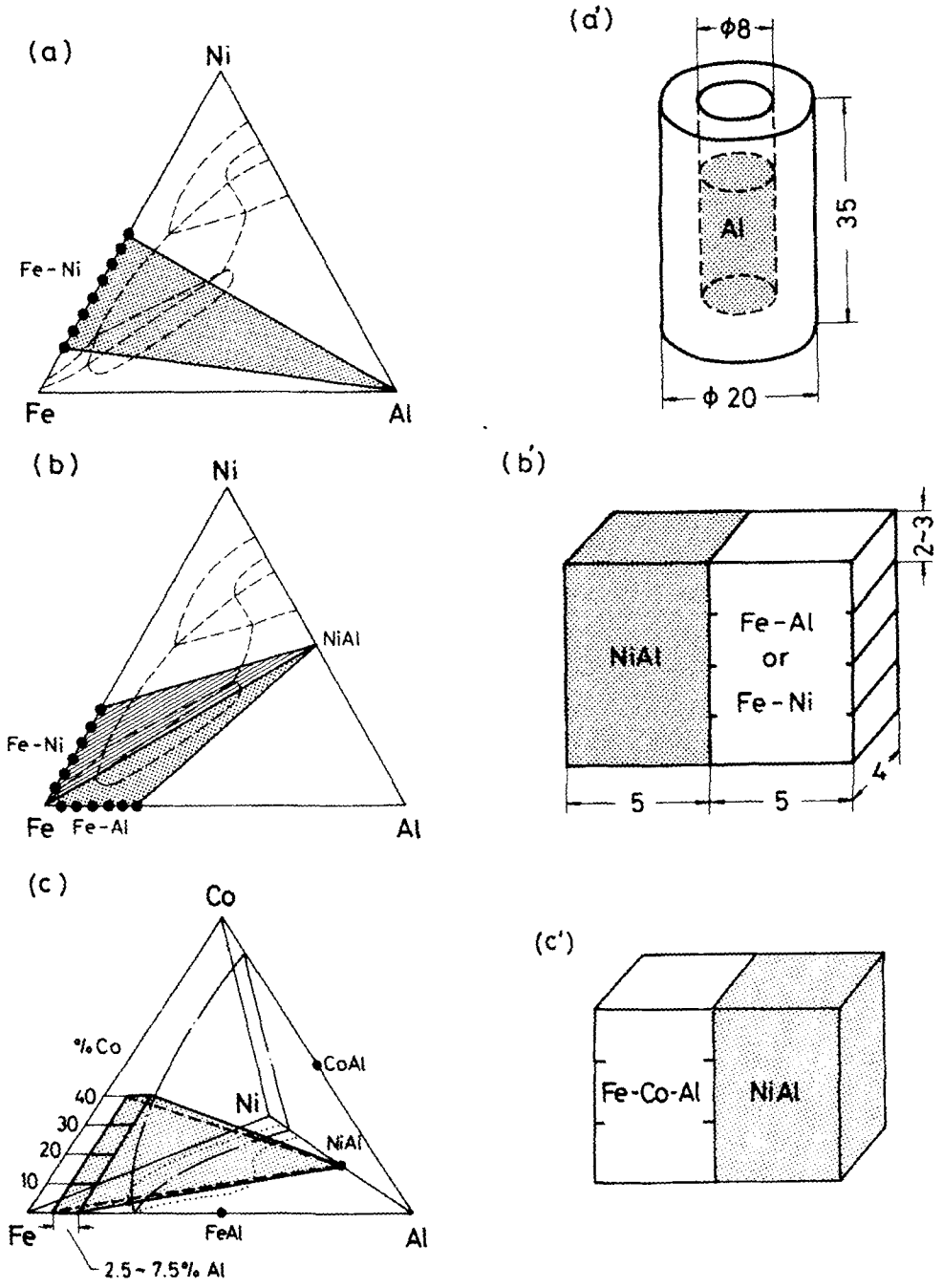

Fig. 3—Scheme of diffusion couples. (*a*) Solid-liquid diffusion couple of Fe-Ni-Al system. (*b*) Solid-solid diffusion couple of Fe-Ni-Al system. (*c*) Solid-solid diffusion couple of Fe-Ni-Al-Co system.

much higher temperature than expected by the regular solution model, and the miscibility gap develops a ridge along the order-disorder transition and Curie temperature lines in both the isothermal and vertical sections.

In the present work, the miscibility gap in Fe-Ni-Al and Fe-Ni-Al-Co systems has been reexamined by the diffusion couple technique in order to prove the above predictions and to provide a substantial basis for further developments of Alnico magnets.

II. EXPERIMENTAL PROCEDURE

The construction of phase diagrams has been facilitated by using the diffusion couple method combined with the electron probe microanalysis.[10] This technique permits acquisition of sufficient data over a wide range of composition from a limited number of diffusion couples.

A. *Preparation of Diffusion Couples*

The alloys of Fe-(5 to 50 at. pct)Ni, Fe-(2.5 to 25 at. pct)Al, Fe-(2.5 at. pct)Al-(10 to 40 at. pct)Co, and NiAl compound were made by induction melting of electrolytic iron (99.95 pct), electrolytic nickel (Ni + Co > 99.95 pct), electrolytic cobalt (99.8 pct), and high purity aluminum (99.9 pct) in desired proportions. Three types of diffusion couples, as illustrated in Figure 3, were prepared, which had been expected to cover the whole range of the miscibility gap in Fe-Ni-Al and Fe-Ni-Al-Co systems. For

Table I. Conversion Parameters, α_{ij}

i \ j	Fe	Ni	Al	Co
Fe	—	0.76	1.18	0.90
Ni	1.10	—	1.90	0.92
Al	2.03	2.30	—	1.88
Co	1.03	1.14	1.39	—

coupling solid specimens together, a special apparatus reported in detail elsewhere[11] was used. These diffusion couples were sealed in transparent quartz capsules under vacuum and held for a long time at fixed temperatures between 850 °C and 1150 °C. The samples were subsequently quenched into ice brine and examined by microscope after cutting into two pieces along the direction of diffusion flux.

B. *Electron Probe Microanalysis of Diffusion Couples*

The determination of concentration profile was carried out by Shimazu ARL-EMX microanalyzer using a LiF crystal for Ni Kα and CO Kα and an ADP crystal for Al Kα radiation. The accelerating voltage for the electron beam and the sample current were kept at 20 KV and 10 nA, respectively. The take-off angle of the spectrometer was 52.5 deg.

The relative intensity of radiation Ki for a component i was converted to the weight fraction Ci according to the following equation proposed by Ziebold and Ogilvie:[12]

$$(1 - Ki)/Ki = \bar{\alpha}_i(1 - Ci)/Ci$$

where $\bar{\alpha}_i$ is the conversion parameter for i-j-k and i-j-k-l systems and is expressed as

$$\bar{\alpha}_i = (\alpha_{ij}Cj + \alpha_{ik}Ck + \alpha_{il}Cl)/(Cj + Ck + Cl)$$

where α_{ij}, α_{ik}, and α_{il} are the conversion parameters for the component i in the binary i-j, i-k, and i-l systems, respectively. The values of α_{ij} were determined by calibration experiments as listed in Table I.

III. RESULTS AND DISCUSSION

A. *Miscibility Gap in Fe-Ni-Al System*

Typical examples of the microstructure and the concentration profile of diffusion couples are shown in Figures 4 and 5, which reveal that α_1 and α_2 phases of different compositions coexist in the couple. The equilibrium composition of each phase is determined by extrapolating the concentration profile to the phase boundary. The results thus obtained for temperatures between 850 and 1150 °C are summarized in Table II.

Figure 6 shows the concentration profile for Fe-20 at. pct Al/NiAl diffusion couple annealed at 900 °C for 400 hours, where no composition gap and phase boundary are observed. This means that the diffusion path in this case does not traverse the two-phase region. As seen in Figure 6, however, there is a singular point which is supposed to occur due to the difference of the diffusivity of atoms in ordered and disordered phases.[13] From such singular points, the critical composition of order-disorder transition at 850 to

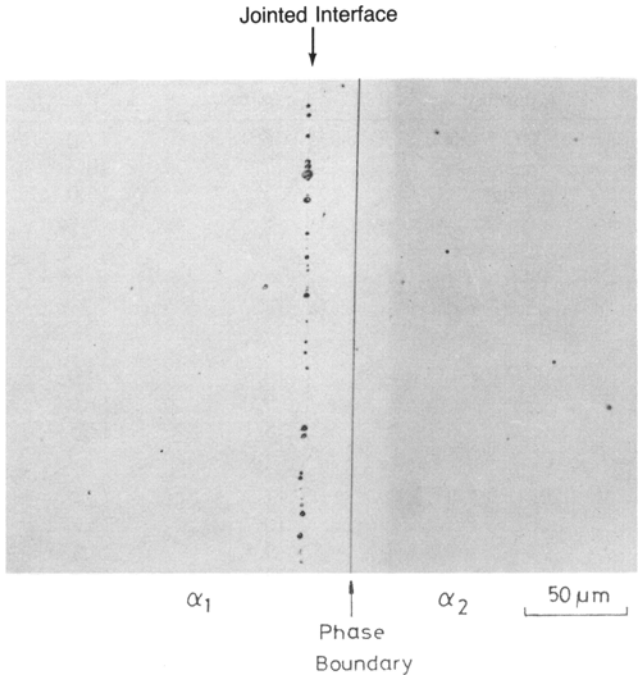

Fig. 4 — Microstructure of Fe-5 at. pct Al/NiAl diffusion couple annealed at 900 °C for 400 h.

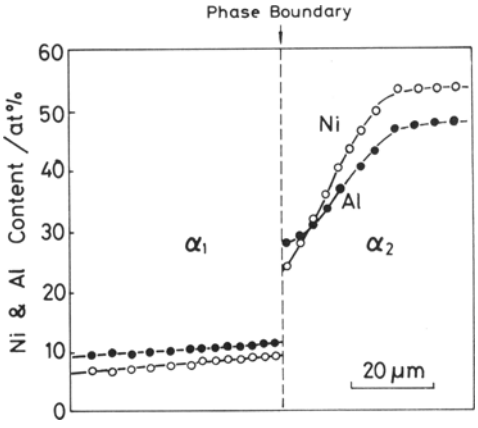

Fig. 5 — Concentration profile for Fe-5 at. pct Al/NiAl diffusion couple annealed at 900 °C for 400 h.

1150 °C has been determined as given in Table III. According to these data, the isothermal section diagrams are obtained as shown in Figure 7. At higher temperatures, the miscibility gap is gradually narrowed and also hidden by the fcc γ phase. The thick broken lines in Figure 7 show the metastable miscibility gap in regions where the γ phase is more stable than either α_1 or α_2.

The miscibility gap in the vertical section through the line XY in Figure 1 is shown in Figure 8. The result is in good agreement with that of Bradley[4] given in Figure 2. However, as discussed in a previous paper,[9] the miscibility gap should develop a ridge along the order-disorder transition line, not only in the vertical section but also in the isothermal section. Thus, the three-dimensional shape of the miscibility gap is similar not to an inverted funnel assumed by Bradley, but to the Napoleon hat as illustrated in Figure 9.

Table II. Equilibrium Composition of Phases in Diffusion Couples for Fe-Ni-Al System

Equilibration	α_1 (bcc, Disorder)		α_2 (bcc, Order)		γ (fcc)	
	At. Pct Ni	At. Pct Al	At. Pct Ni	At. Pct Al	At. Pct Ni	At. Pct Al
850 °C for 600 h	6.9	7.0	38.8	27.8		
	7.4	10.5	38.0	31.8		
	5.5	16.0	25.5	31.5		
	9.1	8.4	37.6	35.9		
			42.5	30.0	12.9	5.8
			43.1	29.2	17.1	4.2
			41.7	28.4	22.2	5.8
			46.8	28.0	29.4	6.4
900 °C for 400 h	6.5	9.0	38.1	30.0		
	9.0	11.0	23.2	27.9		
	8.1	13.5	35.0	31.0		
	7.0	16.0	25.2	30.0		
950 °C for 200 h	11.7	11.6	27.2	23.1		
	10.7	12.8	29.2	26.0		
	9.5	14.1	26.2	25.8		
	8.5	17.0	11.4	20.5		
			37.1	27.6	16.3	7.1
			39.2	27.7	18.6	8.0
			41.3	27.4	22.0	8.0
1000 °C for 150 h	9.0	16.5	11.5	19.0		
	9.5	16.0	14.0	20.0		
	11.5	14.5	24.0	23.0		
	11.8	13.5	23.2	24.0		
1050 °C for 100 *h*	12.7	8.6			10.8	11.2
	15.4	9.5			13.4	13.0
	12.6	14.2	15.0	19.0		
	13.2	14.3	18.2	19.2		
			32.9	24.0	19.9	10.5
			34.1	23.8	19.9	9.2
			41.3	24.0	26.0	9.2
1150 °C for 50 h	14.5	13.4			16.4	10.6
			26.1	19.8	18.2	8.8
			27.5	20.5	21.1	10.0

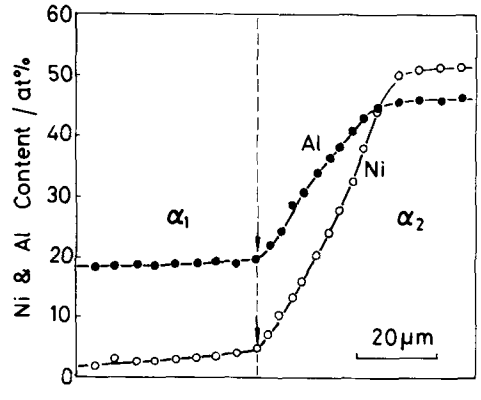

Fig. 6—Concentration profile for Fe-20 at. pct Al/NiAl diffusion couple annealed at 900 °C for 400 h.

Table III. Critical Composition of Order-Disorder Transition in Fe-Ni-Al System

Temperature	At. Pct Ni	At. Pct Al
850 °C	3.3	18.8
	2.5	21.0
900 °C	5.3	18.5
	4.1	20.5
950 °C	4.5	22.5
1000 °C	6.5	20.3
	5.3	22.0
1050 °C	9.0	16.5
1150 °C	10.0	16.3
	13.0	16.5
	14.2	19.7

B. *Miscibility Gap in Fe-Ni-Al-Co System*

Figure 10 shows the concentration profile for Fe-5 at. pct Co/NiAl diffusion couple annealed at 900 °C for 400 hours. It can be seen from this figure that Co atoms concentrate to the NiAl-rich ordered α_2 rather than the Fe-rich disordered α_1. The opposite process was considered to exist on the basis that the saturation magnetization and the Curie temperature of Alnico magnets are raised by the addition of Co. According to the present results, however, more than half of Co

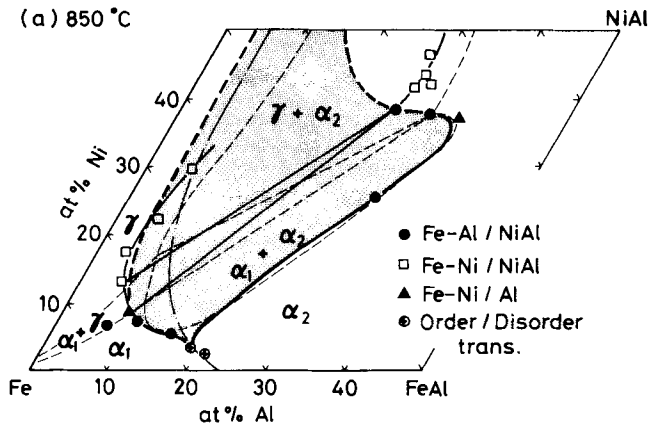

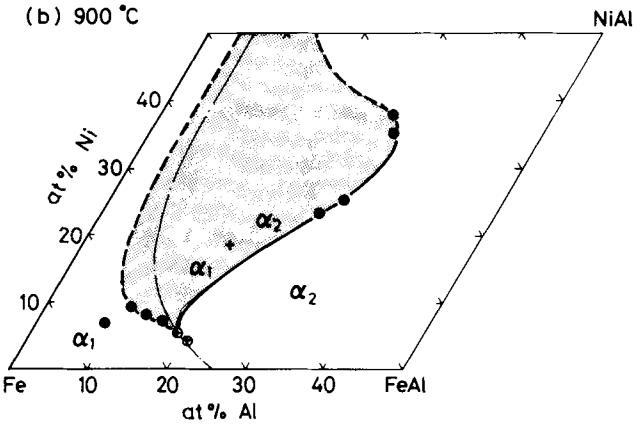

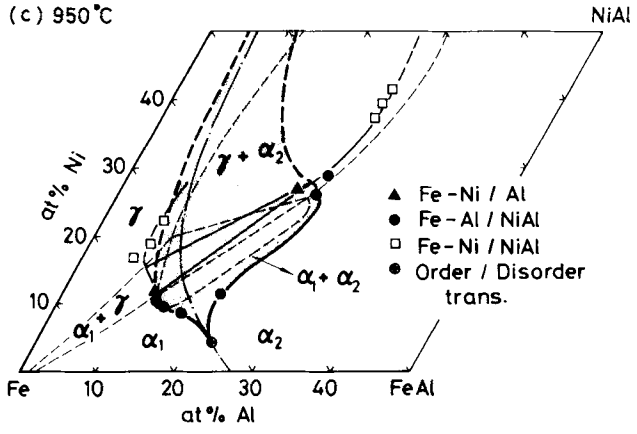

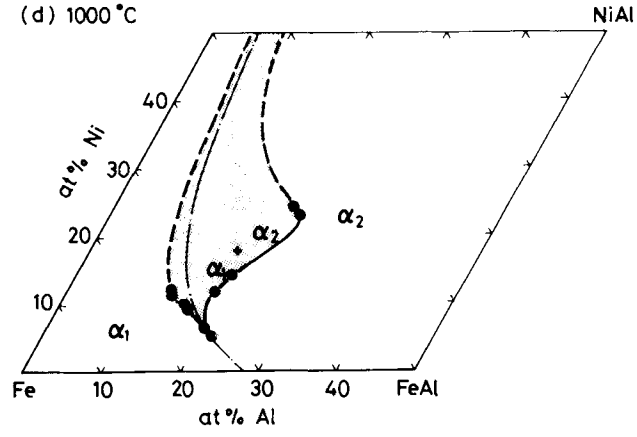

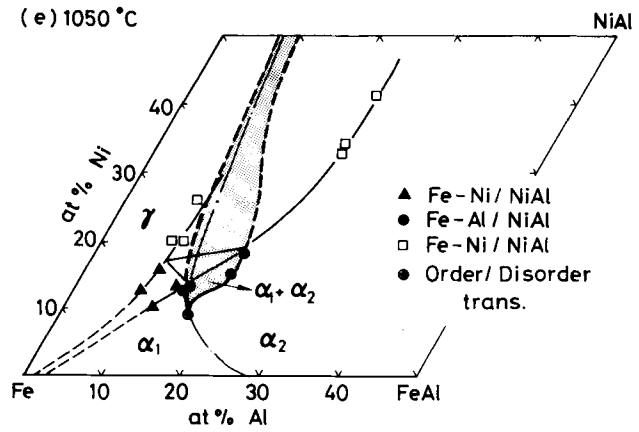

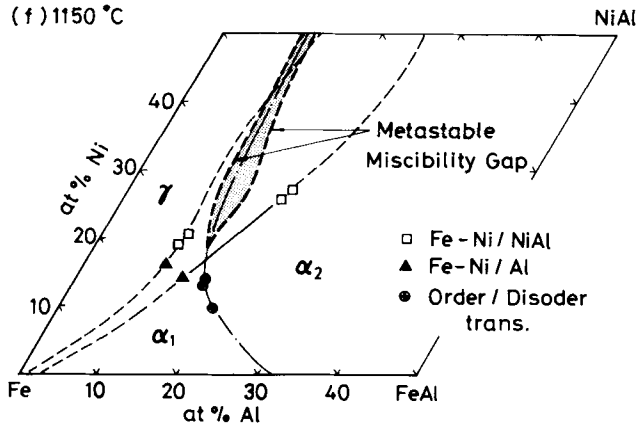

Fig. 7 — Miscibility gap in Fe-Ni-Al system at temperatures between 850 and 1150 °C.

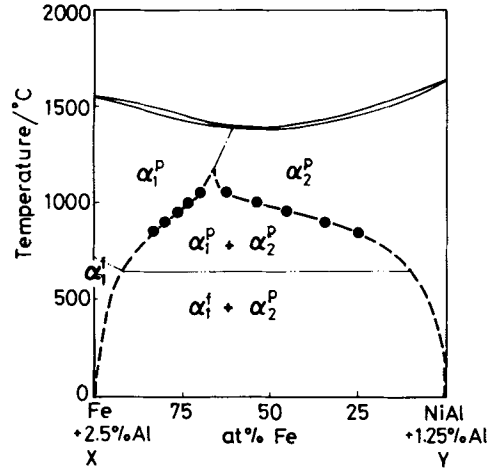

Fig. 8 — Pseudo-binary phase diagram at the same section as Fig. 2.

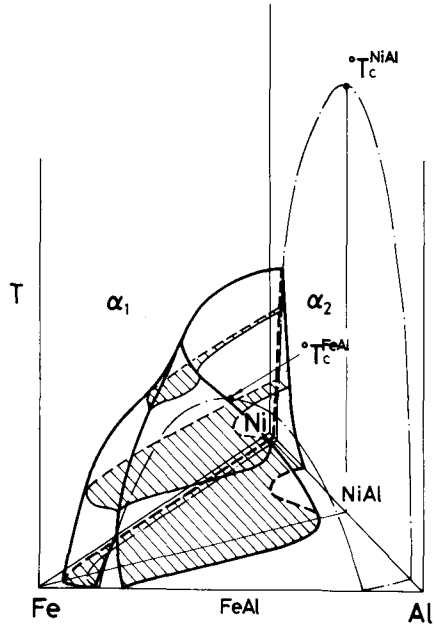

Fig. 9—Three-dimensional illustration of miscibility gap in Fe-Ni-Al system.

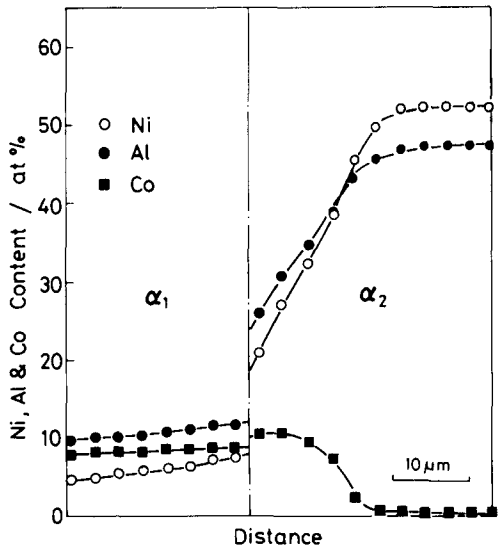

Fig. 10—Concentration profile for Fe-5 at. pct Al-10 at. pct Co/NiAl diffusion couple annealed at 900 °C for 400 h.

Table IV. Equilibrium Composition of Phases in Diffusion Couples for Fe-Ni-Al-Co System

		α_1 (bcc, Disorder)			α_2 (bcc, Order)			γ (fcc)		
Equilibration	No.	At. Pct Ni	At. Pct Al	At. Pct Co	At. Pct Ni	At. Pct Al	At. Pct Co	At. Pct Ni	At. Pct Al	At. Pct Co
850 °C for 600 h	1	6.5	13.5	9.5	19.0	26.0	12.5			
	2	7.0	11.5	9.0	21.5	26.5	11.5			
	3	7.5	11.0	9.0	26.0	29.0	11.0			
	4	5.0	11.0	18.0	8.0	17.0	19.5			
	5	5.0	10.5	17.5	11.0	19.0	19.0			
	6	7.0	9.5	17.0	18.5	23.5	18.0			
	7	5.0	7.0	25.5	18.0	24.5	25.0			
	8	5.5	8.5	26.0	13.0	19.0	27.0			
900 °C for 400 h	1	9.5	11.5	9.0	21.0	23.0	10.0			
	2	8.0	12.5	9.0	17.0	22.0	11.0			
	3	7.5	13.5	9.5	13.0	20.0	11.0			
	4	7.0	11.0	19.0	11.0	17.0	18.5			
	5	7.0	10.0	18.0	14.0	20.0	17.5			
	6	4.5	9.0	27.0	7.0	14.0	26.0			
	7	4.5	7.0	24.5	17.5	22.0	25.5			
	8	4.5	9.0	26.0	7.0	14.0	27.0			
	9	4.5	7.0	25.5	17.5	22.0	24.0			
	10				20.5	24.0	16.0	*	*	*
	11	5.0	7.5	18.0				*	*	*
	12				13.5	22.0	34.5	*	*	*
	13	5.0	7.0	36.5				*	*	*
950 °C for 200 h	1	8.5	13.5	9.0	13.0	17.5	10.0			
	2	9.5	13.0	9.0	14.5	18.0	9.5			
	3	11.0	12.0	9.0	17.0	18.5	9.5			
	4				21.0	23.0	13.5	10.0	8.0	13.0
	5	0.5	4.0	21.0				1.0	3.0	20.0
	6				21.0	23.0	13.5	9.5	7.5	13.0
	7	0.5	3.5	20.5				1.0	3.0	19.5
	8				18.5	21.5	17.0	*	*	*
	9	4.0	8.0	18.0				*	*	*
	10				16.0	19.5	16.0	9.5	8.5	15.5
	11	3.5	7.5	19.0				5.5	6.0	18.5
	12				23.5	26.0	21.0	14.5	12.0	25.5
	13	1.5	5.5	31.0				2.0	3.5	31.0
	14				16.5	23.0	25.0	*	*	*
	15	3.5	8.5	29.0				*	*	*

Table IV. Cont. Equilibrium Composition of Phases in Diffusion Couples for Fe-Ni-Al-Co System

Equilibration	No.	α_1 (bcc, Disorder)			α_2 (bcc, Order)			γ (fcc)		
		At. Pct Ni	At. Pct Al	At. Pct Co	At. Pct Ni	At. Pct Al	At. Pct Co	At. Pct Ni	At. Pct Al	At. Pct Co
	16				20.5	25.0	22.0	*	*	*
	17	3.5	8.5	28.0				*	*	*
	18				23.5	26.0	21.0	14.5	12.0	21.0
	19	1.5	5.5	31.0				2.0	3.5	31.0
	20				17.0	23.0	25.5	*	*	*
	21	3.5	8.5	29.0				*	*	*
	22				20.5	25.0	22.0	*	*	*
	23	4.0	8.5	28.0				*	*	*
	24				7.5	18.5	38.0	*	*	*
	25	5.0	7.0	39.0				*	*	*
	26				16.5	23.5	31.5	*	*	*
	27	4.5	6.5	38.5				*	*	*
	28				15.5	23.5	32.0	10.0	8.0	33.0
	29	2.0	7.0	40.0				3.0	5.5	40.0
	30				18.0	25.0	27.5	12.5	8.0	29.0
	31	2.0	4.0	39.0				2.5	4.5	38.5
1000 °C for 150 h	1				31.0	29.0	7.0	*	*	*
	2	5.0	9.0	9.5				*	*	*
	3				31.0	28.5	7.5	16.5	10.0	7.0
	4	4.0	8.0	9.5				6.5	7.0	9.0
	5				20.0	22.5	18.0	*	*	*
	6	5.0	8.5	19.0				*	*	*
	7				20.0	22.5	16.5	*	*	*
	8	4.0	8.5	18.5				*	*	*
	9				27.0	25.5	12.5	*	*	*
	10	2.0	6.0	19.0				*	*	*
	11				19.5	23.5	20.0	*	*	*
	12	11.0	8.5	20.5				*	*	*
	13				20.0	24.0	20.0	*	*	*
	14	12.0	9.0	21.5				*	*	*
	15				18.0	23.0	22.0	11.5	8.5	22.0
	16	1.0	6.0	29.5				1.7	4.5	29.5
	17				19.5	24.5	22.0	13.0	9.5	21.5
	18	1.5	7.0	29.0				2.0	6.0	29.0
	19				12.5	21.0	32.5	*	*	*
	20	2.0	7.5	39.0				*	*	*
	21				19.5	23.5	26.0	11.5	8.5	27.5
	22				16.0	22.0	27.0	10.0	8.5	28.0

*γ phase was present, but the composition was not determined.

atoms are distributed into the α_2; this is consistent with the fact that the CoAl phase, isomorphous with the NiAl phase, is stable in the Fe-Al-Co system.[14,15,16] The distribution tendency of individual elements between α_1 and α_2 phases is an important factor in considering the role of elements in Alnico magnets, and will be discussed in more detail in a forthcoming paper.[17]

Experimental results on the phase equilibria in Fe-Ni-Al-Co system are summarized in Table IV. The compositions of α_1 and α_2 phases in equilibrium with each other were obtained for various concentrations of Co at 850, 900, and 950 °C. At 900 and 950 °C, the γ phase also takes part in phase equilibria, although the γ phase layer in some diffusion couples was too thin to determine the equilibrium composition. At 1000 °C, the γ phase becomes more stable than either the α_1 or α_2 phase, and the α_1/α_2 equilibrium could not be determined.

As noted above, Co atoms are distributed into the α_2 phase rather than the α_1 phase, but the composition difference between α_1 and α_2 phases is less than 2 at. pct. Therefore, isothermal phase equilibria in Fe-Ni-Al-Co system were constructed on the sections of equiconcentration for Co as shown in Figure 11, supposing that the Co atoms distribute equally to the α_1 and α_2 phases. As seen in Figure 12, the miscibility gap between α_1 and α_2 phases is narrowed and shifted to the Fe-rich corner by the addition of Co. This is because the NiAl-rich α_2 phase is stabilized by dissolving Co, and the order-disorder transition line is shifted to the Fe-rich side. The vertical section diagrams were drawn through the line a′b′ in Figure 11, and the results are shown in Figure 13. The summit of miscibility gap is lowered and shifted to the Fe-rich corner with the increase of Co content. For 40 at. pct Co alloys, it is expected that the miscibility gap has two ridges; one is due to the ordering and the other

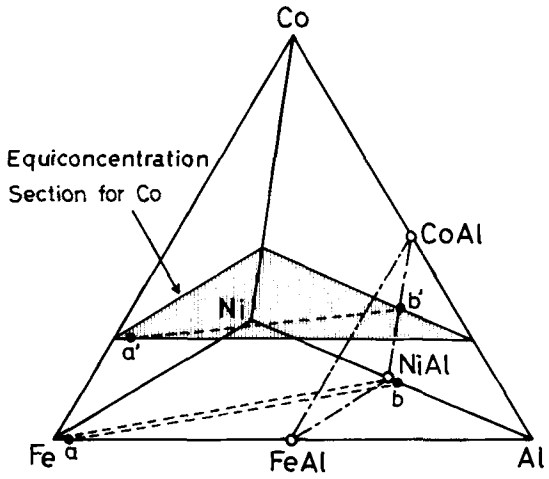

Fig. 11—Equiconcentration section for Co in Fe-Ni-Al-Co system. The pseudo-binary phase diagram is drawn through the line a'b'.

to the magnetic transition as shown in Figure 13(d). On the other hand, the γ phase is somewhat stabilized by the addition of Co, and the γ-loop, with a minimum point similar to that of the Fe-Cr system, appears in the vertical section diagrams. The formation of γ phase spoils the magnetic properties; therefore, the solution treatment of Alnico magnets has been done at temperatures higher than 1200 °C or at intermediate temperatures between 850 and 1000 °C.[18] The reason may be easily understood by the vertical sections given in Figures 13(c) and 13(d).

IV. CONCLUSION

1. The miscibility gap between α_1 (Fe-rich disordered phase) and α_2 (NiAl-rich ordered phase) in the Fe-Ni-Al system develops a ridge along the order-disorder transition line as estimated by thermodynamic calculation.

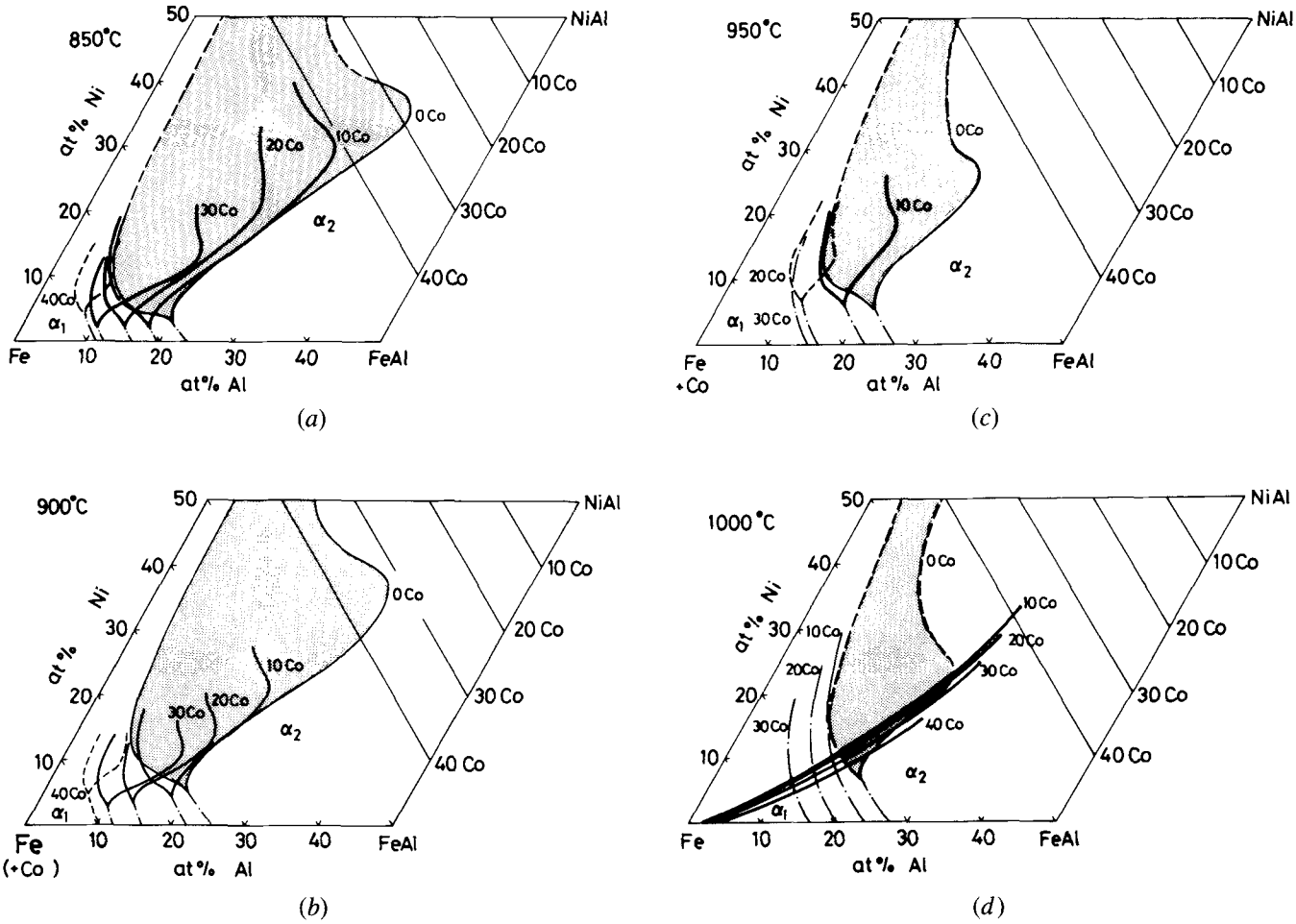

Fig. 12—Miscibility gap in Fe-Ni-Al-Co system between 850 and 1000 °C.

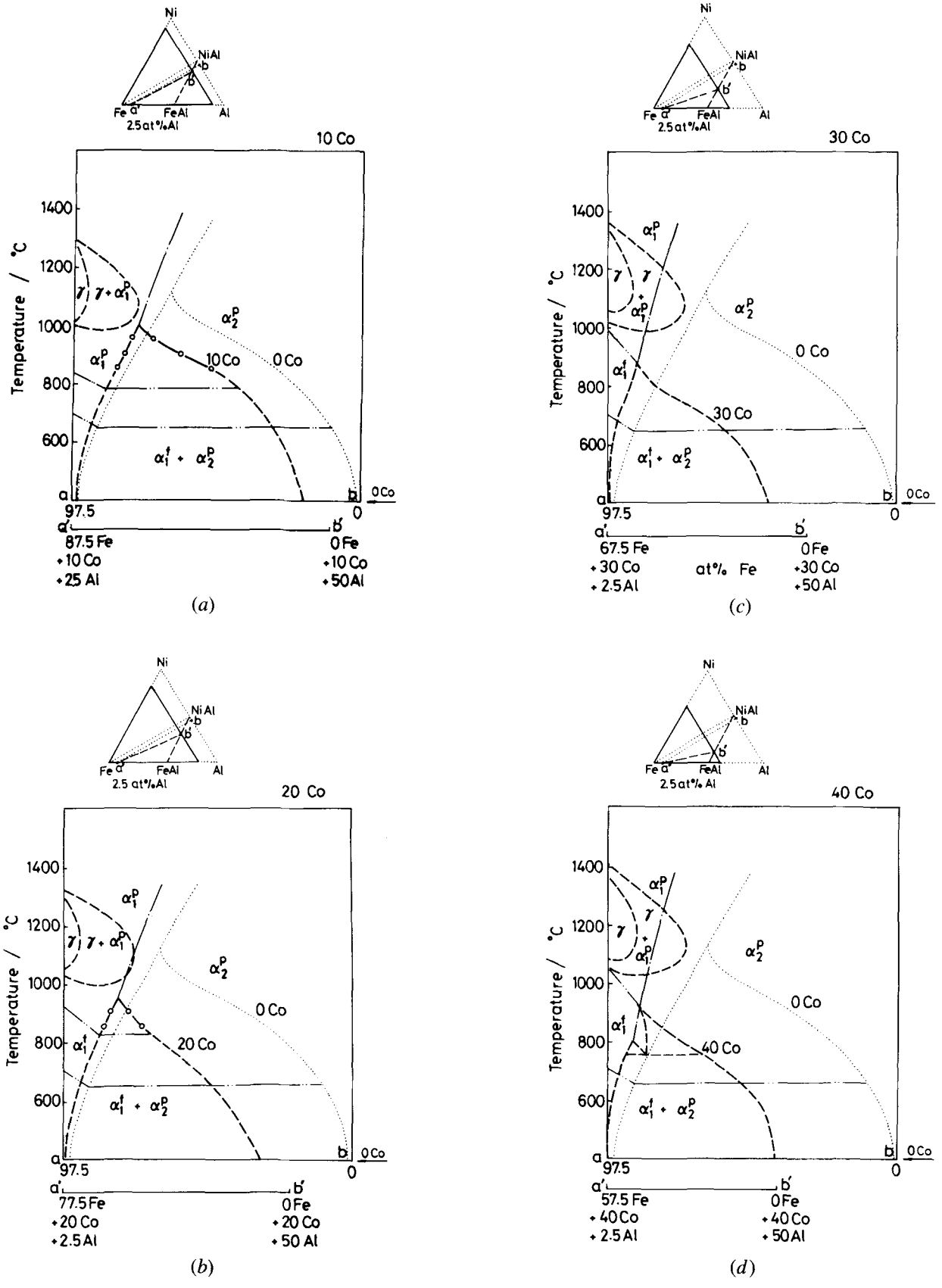

Fig. 13 — Vertical section diagrams at a'-b' in Fe-Ni-Al-Co system. (*a*) 10 at. pct Co, (*b*) 20 at. pct Co, (*c*) 30 at. pct Co, and (*d*) 40 at. pct Co.

2. The three-dimensional shape of the miscibility gap is not an inverted funnel type assumed by Bradley, but is similar to the Napoleon hat.
3. Co concentrates into α_2 rather than α_1, although the compositional difference is not large.
4. The miscibility gap is narrowed and shifted to the Fe-rich corner by the addition of Co, because the α_2 is stabilized and the order-disorder transition point is moved to the Fe-rich side.
5. The fcc γ phase is stabilized by the addition of Co and interferes with the formation of miscibility gap.

ACKNOWLEDGMENTS

The authors wish to express their sincere gratitude to Dr. N. A. Gokcen of United States Bureau of Mines and Professor M. Hillert of Royal Institute of Technology, Stockholm, for reading the manuscript and giving valuable advice.

REFERENCES

1. S. Kiuchi: Rept. of Aeronautical Res. Inst., Tokyo Imp. Univ., 1937, vol. 12, p. 179; 1938, vol. 13, p. 555.
2. A. J. Bradley and A. Taylor: *Nature*, 1938, vol. 140, p. 1012.
3. A. J. Bradley and A. Taylor: *Proc. Roy. Soc., A*, 1938, vol. 166, p. 353.
4. A. J. Bradley: *J. Iron Steel Inst.*, 1949, vol. 163, p. 19; 1951, vol. 168, p. 233; 1952, vol. 171, p. 41.
5. G. Marcon, R. Peffen, and H. Lemaire: *IEEE Trans. Mag.*, 1978, vol. 14, p. 685.
6. J. L. Meijering: Philips Res. Rep., 1950, vol. 5, p. 333; 1951, vol. 6, p. 183.
7. H. K. Hardey: *Acta Metall.*, 1953, vol. 1, p. 210.
8. T. Nishizawa, M. Hasebe, and M. Ko: *Acta Metall.*, 1979, vol. 27, p. 817.
9. T. Nishizawa, S. M. Hao, M. Hasebe, and K. Ishida: *Acta Metall.*, 1983, vol. 31, p. 1403.
10. M. Hasebe and T. Nishizawa: *Applications of Phase Diagrams in Metallurgy and Ceramics*, G. C. Carter, ed., National Bureau of Standards, 1978, p. 911.
11. M. Hasebe, H. Ohtani, and T. Nishizawa: to be published in *Metall. Trans. A*.
12. T. O. Ziebold and R. E. Ogilvie: *Anal. Chem.*, 1963, vol. 35, p. 621.
13. L. A. Girifalco: *Diffusion*, ASM, Metals Park, OH, 1973, p. 185.
14. O. S. Ivanov and M. A. Skryabina: *Izv. Akad. Nauk SSSR*, 1949, p. 242.
15. D. J. Abson and J. A. Whiteman: *Metall. Trans.*, 1972, vol. 3, p. 1157.
16. G. V. Raynor and V. G. Rivlin: *Int. Met. Rev.*, 1982, vol. 27, p. 169.
17. S. M. Hao, K. Ishida, and T. Nishizawa: to be published in *Metall. Trans. A*.
18. Y. Shirakawa, D. Amamiya, and T. Abe: *J. Jap. Inst. Met.*, 1964, vol. 28, p. 313; 1964, vol. 28, p. 689.